New Tripodal Cu(II) Complexes Containing Imidazole Ligands

KENNETH J. OBERHAUSEN, ROBERT J. O'BRIEN, JOHN F. RICHARDSON and ROBERT M. BUCHANAN*
Department of Chemistry, University of Louisville, Louisville, KY 40292 (U.S.A.)
(Received November 20, 1989)

Abstract

A new class of imidazole containing tripodal ligands has been synthesized containing from 0–3 imidazole pendants. Copper(II) complexes of the formulas $[Cu(L)Cl]^+$ and $[Cu(L)(1\text{-MeIm})]^{2+}$ have been prepared and studied by UV–Vis and EPR spectroscopies and cyclic voltammetry. The X-ray crystal structures of $[Cu(bipa)Cl]^+$ and $[Cu(tmima)Cl]^+$ have been determined. Electrochemical and electronic spectral data suggest that the donor strengths of the tripods decrease in the following order: tpa > bpia > bipa > tmima. Results from EPR suggest that the complexes with tmima are more distorted than those of tpa.

Introduction

Histidine is known to be an important biological ligand present at the active site of numerous metalloproteins [1] and it appears to play a particularly crucial role in the coordination chemistry of copper proteins [2]. This observation has stimulated many studies attempting to correlate structure with redox properties of Cu^I and Cu^{II} complexes [3, 4]. In order to assess the electronic factors regulating the stabilization of Cu^I and Cu^{II} forms of copper proteins, tripodal ligands (Fig. 1) containing pyridine [5], pyrazole [6], benzimidazole [7] or imidazole [8] pendant groups have been used as analogs of the imidazole functionality of histidine.

In general, Cu^{II} complexes of tripodal ligands result in the formation of five-coordinate complexes with the ligands occupying four of the five coordination sites. Sterically restricting tripodal ligands, forming five-membered chelate rings, stabilize trigonal bipyramidal complexes with a fifth ligand occupying the apical position *trans* to the amine nitrogen atom [5a, b; 6c]. More flexible ligands forming six-membered chelate rings favor the stabilization of square-pyramidal geometries where the fifth ligand occupies a basal position of the pyramid [5b, c; 6b]. As a result of their greater flexibility, complexes containing six-membered chelate rings favor the stabilization of Cu^I over their five-membered ring analogs. In fact, it has been shown that there is about a 200 mV cathodic shift in the redox potentials of complexes containing five-membered chelate rings relative to their six-membered ring analogs [5b, 9, 10].

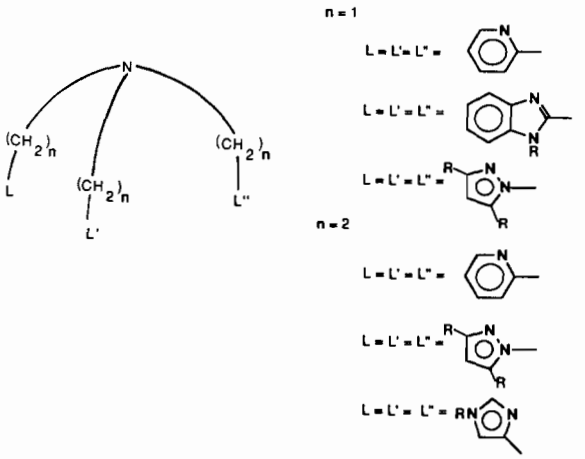

Fig. 1. Tripodal ligands in the literature.

Since few examples of tripodal ligands containing imidazole donors have been reported [7, 8, 11, 12], and the coordination chemistry of this biologically relevant ligand is of interest, we have synthesized several new imidazole containing ligands of the type illustrated in Fig. 2. We have also prepared their corresponding Cl^- and 1-methylimidazole Cu^{II} complexes. We describe herein the results from a detailed structural, spectroscopic and electrochemical study of a series of new tripodal imidazole complexes.

Experimental

Physical Measurements

Absorption spectra were recorded using Shimadzu UV-160 and Perkin-Elmer 330 UV–Vis near-IR spectrophotometers. Proton NMR spectra of the ligands were obtained on a Varian XL-300 spectrometer.

*Author to whom correspondence should be addressed.

0020-1693/90/$3.50

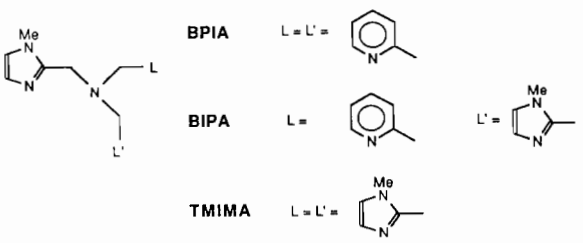

Fig. 2. Tripodal ligands in this study.

EPR spectra were recorded on a Varian E-109 spectrometer equipped with an Oxford Instruments, Inc. cryostat. Electrochemical measurements were obtained in acetonitrile solutions containing 0.1 M tetra-n-butyl ammonium perchlorate using a PAR 175 universal programmer, a PAR 173/178 potentiostat and a digital coulometer interfaced with a Model 2000 X-Y recorder. A three-electrode electrochemical cell, utilizing a Ag/AgCl reference electrode and Pt wire and coil working electrodes, was used for all measurements. The reversibility of the electrochemical processes were evaluated by standard procedures [13], and the formal potentials of the redox couples evaluated using the ferrocene/ferrocenium (Fc/Fc^+) redox couple ($E_{1/2}$ = +0.400 V versus NHE) as an internal standard [14]. Solution susceptibility measurements were obtained in CH_3CN solutions using the Evans method [15].

Reagents

All reagents were commercially available and used as received. All solvents were dried by standard procedures. The ligand tris(2-(pyridyl)methyl)amine (tpa) was prepared by a method previously reported [16], and its purity checked by ^1H and ^{13}C NMR spectroscopies.

Ligand Syntheses

Bis(2-(pyridyl)methyl)(2-(1-methylimidazolyl)-methyl)amine (bpia) (1)

To a stirred suspension of 1-methyl-2-aminomethylimidazole dihydrochloride [17] (2.03 g, 11.0 mmol) and 50 ml of dry acetonitrile was added triethylamine (19.0 ml, 136 mmol) and two equivalents of 2-picolylchloride hydrochloride (3.62 g, 22.0 mmol). The mixture was stirred at room temperature for 24 h after which an additional quantity of 2-picolylchloride hydrochloride (2.82 g, 17.2 mmol) was added. The reaction mixture was then stirred for a further 24 h, filtered to remove the precipitated triethylamine hydrochloride and taken to dryness by rotary evaporation. The resulting oil was dissolved in 50 ml of water. The solution was then made alkaline with $KHCO_3$ and extracted with 3 × 50 ml of methylene chloride. The extracts were combined, dried with $MgSO_4$ and the methylene chloride removed under reduced pressure to give 2.03 g (62.8%) of crude bpia. The crude bpia was dissolved in 30 ml of absolute ethanol, saturated with dry HCl gas and layered with diethyl ether. After cooling to −20.0 °C overnight, bpia hydrochloride precipitated and was collected by filtration. The free base of pure bpia was obtained by dissolving the hydrochloride in an aqueous, alkaline solution and extracting with methylene chloride. Removal of the solvent under reduced pressure gave 1.67 g of 1 (51.8%). ^1H NMR ($CDCl_3$) δ: 3.44 (s, 3H, Im-CH_3), 3.70 (s, 2H, Im-CH_2), 3.74 (s, 4H, Py-CH_2), 6.68 (s, 1H, Im), 6.81 (s, 1H, Im), 7.07 (t, 2H, Py), 7.34 (d, 2H, Py), 7.56 (t, 2H, Py), 8.46 (d, 2H, Py). *Anal.* Calc. for $C_{17}H_{19}N_5$: C, 69.6; H, 6.5; N, 23.9. Found: C, 69.4; H, 6.4; N, 23.8%.

Bis(2-(1-methylimidazolyl)methyl)(2-(pyridyl)-methyl)amine (bipa) (2)

A very dry acetonitrile solution (50 ml) containing bmima [17] (1.846 g, 9 mmol) and triethylamine (6.2 ml, 45 mmol) was stirred for 1 h under a nitrogen atmosphere. Solid 2-picolyl chloride hydrochloride (1.475 g, 9 mmol) was added and the solution stirred for 24 h at room temperature. An additional equivalent of 2-picolylchloride hydrochloride was then added and the solution allowed to stir for a further 24 h. The precipitated triethylamine hydrochloride was filtered and the resulting solution stripped to dryness under reduced pressure. The residue was then dissolved in 30 ml of water. The resulting solution was made alkaline with $KHCO_3$ and extracted with four 30 ml portions of methylene chloride. The combined extracts were then dried with $MgSO_4$ and the methylene chloride removed under reduced pressure to yield 1.63 g (61%) of 2. ^1H NMR ($CDCl_3$) δ: 3.34 (s, 6H, Im-CH_3), 3.76 (s, 4H, Im-CH_2), 3.82 (s, 2H, Py-CH_2), 6.78 (s, 2H, Im-CH), 6.92 (s, 2H, Im-CH), 7.15 (t, 1H, Py), 7.23 (d, 1H, Py), 7.61 (t, 1H, Py), 8.52 (d, 1H, Py). *Anal.* Calc. for $C_{16}H_{20}N_6$: C, 64.8; H, 6.8; N, 28.4. Found: C, 64.4; H, 6.6; N, 28.0%.

Tris(2-(1-methylimidazolyl)methyl)amine (tmima) (3)

This compound was prepared analogously to 2 using two equivalents of 2-chloromethyl-1-methylimidazole hydrochloride [18]. The yield was 1.66 g (62%) of 3. ^1H NMR ($CDCl_3$) δ: 3.03 (s, 9H, Im-CH_3), 3.78 (s, 6H, Im-CH_2), 6.74 (s, 3H, Im-CH), 6.88 (s, 3H, Im-CH). *Anal.* Calc. for $C_{15}H_{21}N_7 \cdot H_2O$: C, 56.8; H, 7.3; N, 30.9. Found: C, 56.4; H, 7.3; N, 30.6%.

Syntheses of Metal Complexes

[Cu(bpia)Cl]PF_6 (4)

To a stirred solution of bpia (0.50 g, 1.7 mmol) in 10 ml of methanol was added $CuCl_2 \cdot 2H_2O$ (0.29 g,

1.7 mmol). The resulting dark green solution was stirred for 5 min and NH_4PF_6 (0.28 g, 1.7 mmol) was added to precipitate the complex as a light green powder. Recrystallization from methanol gave 0.70 g (75%) of [Cu(bpia)Cl]PF_6 (**4**). *Anal.* Calc. for $CuC_{17}H_{19}N_5ClPF_6$: C, 38.0; H, 3.6; N, 13.0. Found: C, 37.8; H, 3.5; N, 13.0%.

[Cu(bipa)Cl]$PF_6 \cdot CH_3CN$ (5)

Compound **5** was prepared in an 86% yield by the same procedure used to prepare **4** and recrystallized from a 2:1 CH_3OH/CH_3CN solution. *Anal.* Calc. for $CuC_{18}H_{23}N_7ClPF_6$: C, 37.2; H, 4.0; N, 16.9. Found: C, 37.1; H, 3.8; N, 16.8%.

[Cu(tmima)Cl]PF_6 (6)

Compound **6** was also prepared by the same procedure used to prepare **4** and recrystallized from a CH_3OH/CH_3CN solution (93% yield). *Anal.* Calc. for $CuC_{15}H_{21}N_7ClPF_6$: C, 33.2; H, 3.9; N, 18.1. Found: C, 32.7; H, 3.7; N, 17.7%.

[Cu(bpia)(1-MeIm)]$(PF_6)_2$ (7)

A solution of 1-methylimidazole (0.12 g, 1.5 mmol) and 8 ml of methanol was added with stirring to a suspension of [Cu(bpia)Cl]PF_6 (0.40 g, 0.74 mmol) in 10 ml of methanol. The mixture was stirred for 30 min giving a blue solution. The addition of NH_4PF_6 (0.12 g, 0.74 mmol) gave 0.39 g (72%) of [Cu(bpia)(1-MeIm)]$(PF_6)_2$ (**7**) as a light blue powder. Recrystallization from CH_3OH gave crystals suitable for analysis. *Anal.* Calc. for $CuC_{21}H_{25}N_7P_2F_{12}$: C, 34.6; H, 3.5; N, 13.5. Found: C, 34.6; H, 3.4; N, 13.5%.

[Cu(bipa)(1-MeIm)]$(PF_6)_2$ (8) and
[Cu(tmima)(1-MeIm)]$(PF_6)_2$ (9)

Complexes **8** and **9** were prepared in reactions analogous to that used to prepare **7** giving yields of 86% and 88%, respectively. These two complexes were recrystallized from 1:1 CH_3OH–CH_3CN. *Anal.* Calc. for **8**, $CuC_{20}H_{26}N_8P_2F_{12}$: C, 32.8; H, 3.6; N, 15.3. Found: C, 32.8; H, 3.6; N, 15.3%. Calc. for **9**, $CuC_{19}H_{27}N_9P_2F_{12}$: C, 31.1; H, 3.7; N, 17.2. Found: C, 31.0; H, 3.6; N, 17.1%.

X-ray Diffraction

A summary of the crystal data, the experimental details and the results of the structure refinement are listed in Table 1. X-ray diffraction intensity data were collected on an Enraf-Nonius CAD-4 diffractometer at 295(1) K using the ω–2θ scan technique to maximum 2θ values of 52° for complexes **5** and **6**. As a check of crystal and electronic stability three representative reflections were measured every hour of X-ray exposure. The intensities of these reflections decreased throughout the data collection (−8.6%) for complex **6** and a linear decay correction was applied.

TABLE 1. Crystal data for complexes **5** and **6**

Formula	$CuC_{16}H_{20}N_6ClPF_6$	$CuC_{17}H_{24}N_8ClPF_6$
Formula weight	540.34	584.39
Crystal dimensions	0.2 × 0.3 × 0.5	0.45 × 0.45 × 0.5
Space group	$P2_1/n$	$P\bar{1}$
a (Å)	13.361(2)	12.766(1)
b (Å)	12.665(3)	12.910(2)
c (Å)	13.376(3)	8.900(1)
α (°)	90	107.58(1)
β (°)	106.33(2)	96.82(1)
γ (°)	90	61.65(1)
V (Å^3)	2172.2	1230.0
μ (cm^{-1})	12.7	11.3
Z	4	2
ρ_{calc} (g cm^{-1})	1.65	1.58
ρ_{obs} (g cm^{-1})	1.65(1)	1.57(1)
Temperature (°)	23(1)	23(1)
Radiation, λ (Å)	Mo Kα (0.71073)	Mo Kα (0.71073)
Scan technique	ω–2θ	ω–2θ
Monochromator	graphite	graphite
No. unique reflections	4207	4805
No. observed	3018 ($I > 3\sigma(I)$)	4240 ($I > 3\sigma(I)$)
GOF	1.05	1.09
R	0.040	0.039
R_w	0.043	0.044

The intensities of these reflections did not decrease for complex **5**. All data were corrected for Lorentz and polarization effects and empirical absorption corrections based on series of psi scans were applied to each data set. Relative transmission coefficients ranged from 0.950 to 1.000 for complex **5** and from 0.910 to 0.998 for **6**. All data were processed and the crystal structures solved using the SDP package [19]. All calculations were performed on a VAX-11/750 computer using SDP/VAX. The copper atom position in **5** was located using MULTAN, while in **6** the copper atom was located using the Patterson method. The remaining atoms of the complexes were located using successive least-squares and difference Fourier syntheses. The structures were refined using full-matrix least-squares techniques where the function minimized in each case was $\Sigma w(|F_o| - |F_c|)^2$ and the weighting factors $w = [\sigma(F)^2 + (0.01F)^2 + 0.40]^{-1}$ for **5**, and $w = [\sigma(F)^2 + (0.01F)^2 + 0.30]^{-1}$ for **6**, were taken from Killean and Lawrence [20] and used in the final cycles. Scattering factors were taken from Cromer and Waber [21] and anomalous dispersion effects [22] were included in F_c with the values for $\Delta f'$ and $\Delta f''$ being those of Cromer [23]. Final agreement factors for **5** were found to be $R = \Sigma(||F_o| - |F_c||)/\Sigma|F_o| = 0.040$ and $R_w = [\Sigma w(|F_o| - |F_c|)^2/\Sigma w|F_o|^2]^{1/2} = 0.043$ for 315 parameters and 3018 ($I > 3\sigma(I)$) reflections, while those for **6** were 0.039 and 0.044 for 292 parameters and 4240 ($I > 3\sigma(I)$) reflections. The final peak in the difference Fourier of **5** had a height of

TABLE 2. Table of positional parameters for $[Cu(bipa)Cl]^+$

Atom	x	y	z	B (Å^2)
Cu	0.26738(3)	0.22679(4)	0.67805(3)	3.330(9)
Cl	0.21860(8)	0.30465(9)	0.80631(8)	4.84(2)
N1	0.3167(2)	0.1592(2)	0.5547(2)	3.25(7)
N2	0.1285(2)	0.1760(3)	0.5889(2)	3.71(7)
N3	0.0332(3)	0.1224(3)	0.4357(3)	4.05(8)
N4	0.3853(2)	0.1369(2)	0.7615(2)	3.45(7)
N5	0.4895(2)	0.0030(2)	0.7644(3)	4.03(7)
N6	0.3054(2)	0.3647(2)	0.6053(2)	3.58(7)
C1	0.2264(3)	0.1508(3)	0.4597(3)	3.99(9)
C2	0.1300(3)	0.1471(3)	0.4944(3)	3.47(8)
C3	0.0258(3)	0.1691(3)	0.5914(3)	4.2(1)
C4	−0.0335(3)	0.1358(3)	0.4969(4)	4.6(1)
C5	0.0045(4)	0.0924(4)	0.3262(4)	5.6(1)
C6	0.3629(3)	0.0547(3)	0.5912(3)	3.91(9)
C7	0.4139(3)	0.0638(3)	0.7046(3)	3.46(8)
C8	0.4447(3)	0.1217(3)	0.8628(3)	4.09(9)
C9	0.5101(3)	0.0394(3)	0.8648(3)	4.5(1)
C10	0.5416(3)	−0.0869(4)	0.7311(4)	6.1(1)
C11	0.3967(3)	0.2328(3)	0.5362(3)	3.74(8)
C12	0.3598(3)	0.3447(3)	0.5371(3)	3.66(9)
C13	0.2741(3)	0.4640(3)	0.6136(3)	4.6(1)
C14	0.2946(4)	0.5452(4)	0.5553(4)	5.8(1)
C15	0.3483(4)	0.5231(4)	0.4844(4)	6.4(1)
C16	0.3821(4)	0.4218(4)	0.4740(4)	5.0(1)
P	−0.2747(1)	0.1677(1)	0.6762(1)	4.92(3)

Anisotropically refined atoms are given in the form of the isotropic equivalent displacement parameter.

0.42(10) e/Å^3 associated with the disordered PF_6 molecule. In **6** the final peak had a height of 0.64(10) e/Å^3 associated with the CH_3CN solvate molecule. Positional parameters for complexes **5** and **6** are located in Tables 2 and 3, respectively.

TABLE 3. Table of positional parameters for $[Cu(tmima)Cl]^+$

Atom	x	y	z	B (Å^2)[a]
Cu	0.81877(3)	0.82612(3)	0.95890(5)	3.095(8)
Cl	0.80834(9)	0.77439(8)	0.6964(1)	4.59(2)
P	1.24179(9)	0.67722(8)	0.4501(1)	4.33(2)
F1	1.2015(3)	0.6656(2)	0.2746(3)	7.30(8)
F2	1.2752(3)	0.6984(3)	0.6291(3)	8.7(1)
F3	1.1712(3)	0.6109(2)	0.4727(4)	8.88(8)
F4	1.3571(3)	0.5537(3)	0.4027(4)	10.3(1)
F5	1.3090(2)	0.7482(2)	0.4273(4)	7.83(8)
F6	1.1232(2)	0.8051(2)	0.4981(4)	7.34(9)
N1	0.8305(2)	0.8814(2)	1.2131(3)	3.10(6)
N2	0.9802(2)	0.8287(2)	0.9807(3)	3.27(6)
N3	1.0964(2)	0.8983(2)	1.1281(3)	3.61(6)
N4	0.8292(2)	0.6791(2)	1.0094(3)	3.10(6)
N5	0.8788(2)	0.5681(2)	1.1750(3)	3.34(6)
N6	0.6716(2)	0.9894(2)	1.0122(3)	3.67(7)
N7	0.5409(2)	1.1422(3)	1.1886(4)	4.38(8)
N8	0.4062(4)	0.2494(4)	0.7115(6)	8.9(1)*
C1	0.9031(3)	0.9478(3)	1.2510(4)	3.35(7)
C2	0.9947(3)	0.8906(2)	1.1220(4)	3.11(7)
C3	1.0773(3)	0.7945(3)	0.8908(4)	3.73(8)
C4	1.1505(3)	0.8363(3)	0.9810(4)	4.04(8)
C5	1.1399(3)	0.9639(3)	1.2643(5)	4.84(9)
C6	0.8874(3)	0.7697(3)	1.2694(4)	3.53(8)
C7	0.8630(3)	0.6731(2)	1.1535(4)	2.95(7)
C8	0.8219(3)	0.5724(3)	0.9329(4)	3.43(8)
C9	0.8523(3)	0.5039(3)	1.0343(4)	3.77(8)
C10	0.9175(4)	0.5285(3)	1.3177(4)	4.8(1)
C11	0.7071(3)	0.9640(3)	1.2774(4)	3.71(8)
C12	0.6403(3)	1.0341(3)	1.1625(4)	3.49(8)
C13	0.5882(3)	1.0710(3)	0.9366(5)	4.30(9)
C14	0.5075(3)	1.1656(3)	1.0465(5)	5.1(1)
C15	0.4788(4)	1.2207(5)	1.3407(6)	6.6(1)
C16	0.4202(7)	0.4529(7)	0.781(1)	11.7(2)*
C17	0.4141(5)	0.3368(5)	0.7448(7)	7.5(1)*

[a]Starred atoms were refined isotropically. Anisotropically refined atoms are given in the form of the isotropic equivalent displacement parameter.

Results and Discussion

Synthesis

Several imidazole containing tripodal ligands have been synthesized and used to prepare two series of Cu(II) complexes. The ligands bpia (**1**) and bipa (**2**) were synthesized by reacting 2-picolylchloride hydrochloride with 1-methyl-2-aminomethylimidazole [17] and bmima [17], respectively, in acetonitrile containing triethylamine. The ligand tmima (**3**) was prepared under similar conditions using 2-chloromethyl-1-methylimidazole hydrochloride [18] and bmima [17]. Complexes **4**–**6**, which have the general formula $[Cu(L)Cl]PF_6$ (where L = bpia, bipa and tmima), were prepared by the reaction of **1**–**3** with stoichiometric amounts of $CuCl_2 \cdot 2H_2O$ in methanol. Addition of NH_4PF_6 to the resulting green solutions caused an immediate precipitation of microcrystalline samples of the complexes. Recrystallization of complexes **5** and **6** from methanol/acetonitrile solutions gave crystals suitable for X-ray structural analyses. For **5**, crystals left in the recrystallization solution turned opaque after 24 h. Analysis of the sample indicated the acquisition of an acetonitrile solvate molecule, which was not lost on extended vacuum drying, unlike that found for **6**. Complexes **7**–**9** were prepared by reacting compounds **4**–**6** with a slight excess of 1-methylimidazole in methanol. Addition of NH_4PF_6 to the blue solutions resulted in the precipitation of the complexes in yields exceeding 70%. Recrystallization of these complexes, which have the general formula $[Cu(L)(1\text{-MeIm})](PF_6)_2$, gave analytically pure compounds. The compounds $[Cu(tpa)Cl]^+$ [5b, 10] and $[Cu(tpa)(1\text{-MeIm})]^{2+}$ [10] were prepared by analogous procedures used to prepare compounds **4**–**9**.

Description of the Structures

[Cu(bipa)Cl]PF_6 (5)

Compound 5 crystallizes in the monoclinic space group $P2_1/n$. An ORTEP plot of the cation is illustrated in Fig. 3. Selected bond lengths and angles are given in Table 4. The cation has a distorted trigonal bipyramidal geometry similar to that reported previously for $[Cu(tpa)Cl]^+$ [5b]. The copper atom is bonded to two imidazole ring nitrogens (N2 and N4), a pyridine ring nitrogen (N6), a tertiary amine nitrogen (N1) and a chloride ion. The trigonal plane of the molecule is formed by atoms N2, N4 and N6. The chloride ion and N1 atom occupy apical positions of the trigonal bipyramid. The Cu–Cl bond length is 2.229(2) Å, close to the value of 2.233(2) Å reported for the structurally similar $[Cu(tpa)Cl]^+$ complex [5b] (Table 4). The Cu–N1 bond length (2.121(3) Å), however, is nearly 0.07 Å longer than the Cu–N1 length reported for $[Cu(tpa)Cl]^+$ (2.050(6) Å), suggesting that 5 is more highly distorted. This distortion is reflected in the values of the shape determining angles, $e_1 = 49.51$, $e_2 = 45.36$, $e_3 = 57.57°$, compared to those in $[Cu(tpa)Cl]^+$, $e_1 = 53.0$, $e_2 = 51.3$, $e_3 = 52.6°$. An ideal trigonal bipyramid has angles of 53.1°, for e_1, e_2 and e_3, as defined by Muetterties and Guggenberger [24]. The Cu–N(imidazole) bond lengths average 2.009 Å, close to values reported below for $[Cu(tmima)Cl]PF_6$ (6) and somewhat longer than the Cu^{II}–N(imidazole) bond distances found in other Cu^{II}–imidazole complexes [25]. The Cu–N(pyridine) bond length is significantly longer (2.129(3) Å) than the average Cu–N(pyridine) length reported for $[Cu(tpa)Cl]^+$ (2.065(7) Å) [5b], but lies intermediate between the average basal Cu–N(pyridine) bond lengths and the apical Cu–N(pyridine) bond lengths reported for the square-pyramidal complexes $[Cu(tepa)NO_3]^+$ [5c, 10], $[Cu(tepa)Cl]^+$ [5b, 10] and $[Cu(tepa)(1\text{-MeIm})]^{2+}$ [10]. A very long Cu–N(pyrazole) bond length of 2.193(3) Å is observed in $[Cu(amtp)NO_3]^+$ [6c] (amtp is the tris-3,5-dimethylpyrazole tripod ligand).

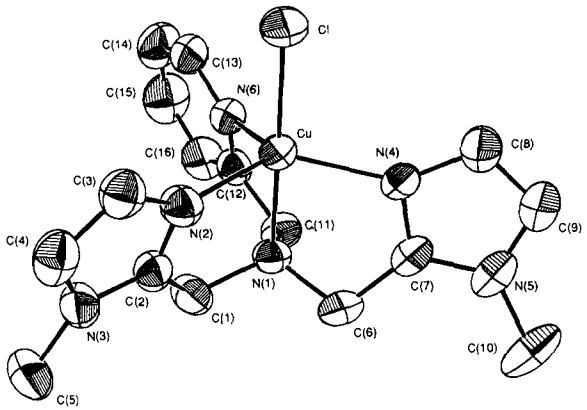

Fig. 3. ORTEP drawing of $[Cu(bipa)Cl]^+$.

Further distortions in the coordination geometry of 5 are reflected in the reduced N1–Cu–N2, N1–Cu–N4 and N1–Cu–N6 bond angles, which deviate significantly from 90° (Table 4). These chelate bond angles average 80.3(1)°, reflecting the constraining nature of the ligand. In $[Cu(tpa)Cl]^+$, the angles are slightly less constrained averaging 81.1(1)° [5b]. The greater distortion in 5 is associated with the atoms in the trigonal plane. Bond angles within the trigonal plane are 106.9(1), 117.9(1) and 126.7(1)° rather than 120°, as expected. The trigonal bond angles in $[Cu(tpa)Cl]^+$ are statistically closer to 120° averaging 117.9(1)°. In $[Cu(amtp)NO_3]^+$ [6c], the trigonal angles are 105.1(1), 106.5(1) and 140.7(1)°, similar to the angles reported for 5.

TABLE 4. Selected bond lengths (Å) and angles (°) for complexes 5 and 6

	5	6	$[Cu(tpa)Cl]^+$ [a]
Cu–N1	2.121(3)	2.167(3)	2.050(6)
Cu–N2	2.009(3)	2.062(3)	2.062(8)(pyN2)
Cu–N4	2.009(3)	2.021(4)	2.060(9)(pyN3)
Cu–N6	2.129(3)(pyN)	2.011(2)	2.072(6)(pyN4)
Cu–Cl	2.229(1)	2.234(1)	2.233(2)
N1–Cu–N2	81.2(1)	79.0(1)	81.5(4)
N1–Cu–N4	80.6(1)	80.1(2)	81.1(4)
N1–Cu–N6	79.1(1)	79.9(1)	80.8(3)
N1–Cu–Cl	177.43(9)	177.9(1)	179.1(4)
N2–Cu–N4	126.7(1)	112.0(2)	118.2(3)
N2–Cu–N6	106.9(1)	116.9(1)	118.8(3)
N4–Cu–N6	117.9(1)	121.6(1)	116.0(3)
Cl–Cu–N2	100.3(2)	99.6(1)	97.6(3)
Cl–Cu–N4	100.1(1)	101.9(1)	99.6(3)
Cl–Cu–N6	98.5(1)	99.4(1)	99.4(2)

[a]Ref. 10.

[Cu(tmima)Cl]$PF_6 \cdot CH_3CN$ (6)

Compound **6** represents the first tripodal imidazole complex of Cu^{II} to be studied crystallographically. The compound crystallizes in the triclinic space group $P\bar{1}$. An ORTEP plot of the cation is illustrated in Fig. 4. Selected bond lengths and angles are given in Table 4 along with those of complex **5** and $[Cu(tpa)Cl]^+$ [5b]. The cupric atom in **6** is bonded to the three imidazole nitrogen atoms of tmima, N2, N4 and N6, as well as a tertiary amine nitrogen (N1) and a chloride ion. The geometry around the copper center is best described as a distorted trigonal bipyramid [24] with $e_1 = 47.51$, $e_2 = 53.97$, $e_3 = 48.51°$. As with **5**, the greatest distortions are associated with the chelate angles, which average 79.6°. The distortion is also reflected in the lengthening of the Cu–N1 bond distance. In **6**, the Cu–N1 length is 2.167(3) Å, which is 0.12 Å longer than the Cu–N1 bond distance reported for $[Cu(tpa)Cl]^+$, and approximately 0.05 Å longer than that found for **5**. The Cu–Cl bond distance, on the other hand, is 2.234(1) Å, consistent with the values reported earlier for **5** and $[Cu(tpa)Cl]^+$ [5b]. The Cu–N(imidazole) bond lengths vary from 2.011(2) to 2.062(3) Å, being somewhat longer than Cu–N(imidazole) lengths reported previously for **5** and other Cu^{II}–imidazole complexes [25]. As a result of the strained configuration of the complex, the metal has been displaced 0.363 Å from the trigonal plane towards the chloride ion. In $[Cu(tpa)Cl]^+$ the geometry is less distorted and the copper is displaced only 0.319 Å from the trigonal plane. In **5**, the copper ion is displaced 0.343 Å, a value intermediate between that found for **6** and $[Cu(tpa)Cl]^+$.

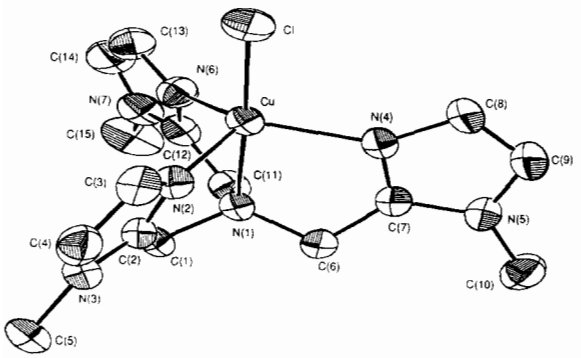

Fig. 4. ORTEP drawing of $[Cu(tmima)Cl]^+$.

Electronic Spectroscopy

The electronic spectral properties of compounds **4–9**, in acetonitrile solutions, are listed in Table 5 along with the data for $[Cu(tpa)Cl]PF_6$ [5b, 10] and $[Cu(tpa)(1\text{-MeIm})](PF_6)_2$ [10]. The high energy transitions observed between 250 and 300 nm are assigned to various ligand to metal charge transfer transitions [25d]. In the series of $[Cu(L)Cl]^+$ complexes, the intensity of the band at 260 nm decreases as 1-methylimidazole pendants are substituted for pyridine pendants. For $[Cu(bpia)Cl]^+$ the band is relatively intense ($\epsilon = 8250$ M^{-1} cm^{-1}), while in $[Cu(bipa)Cl]^+$ the absorption is much weaker ($\epsilon = 4510$ M^{-1} cm^{-1}). In $[Cu(tmima)Cl]PF_6$, this band is completely obscured by a more intense transition at 288 nm ($\epsilon = 4560$ M^{-1} cm^{-1}). A similar trend is observed in the spectra of the $[Cu(L)(1\text{-MeIm})]^{2+}$ complexes: $[Cu(bpia)(1\text{-MeIm})]^{2+}$ (256 nm, $\epsilon = 9430$ M^{-1} cm^{-1}), $[Cu(bipa)(1\text{-MeIm})]^{2+}$ (261 nm, $\epsilon = 5590$ M^{-1} cm^{-1}) and $[Cu(tmima)(1\text{-MeIm})]^{2+}$ (268 nm, $\epsilon = 2250$ M^{-1} cm^{-1}).

The copper complexes in general give rather broad spectra in the visible and near-IR regions (Fig. 5(a) (b)). They exhibit a single absorption band with a high energy shoulder typical of trigonal bipyramidal Cu^{II} complexes [5b, 7c, 26], supporting the retention of the solid-state structures of **5** and **6** in solution.

There is an apparent trend in the spectral properties of compounds **4–6** related to the ligand field strength of the tripodal ligand. As the pyridine pendants of $[Cu(tpa)Cl]^+$ are replaced with imidazole ligands, the absorption maxima of the complexes shift progressively to lower energies. For $[Cu(tmima)Cl]^+$ (**6**), the absorption maximum occurs at 1123 nm ($\epsilon = 112$ M^{-1} cm^{-1}) while the high energy shoulder is centered at 830 nm ($\epsilon = 98$ M^{-1} cm^{-1}). In $[Cu(tpa)-$

TABLE 5. UV–Vis data for the complexes[a, b]

Complex	$\lambda_{max}(\epsilon)$	$\lambda_{max}(\epsilon)$	$\lambda_{max}(\epsilon)$	$\lambda_{max}(\epsilon)$
$[Cu(tpa)Cl]PF_6$ [c]	962 (201)	736 (92)	294(sh) (3430)	257 (12200)
$[Cu(bpia)Cl]PF_6$ (**4**)	1003 (141)	780 (71)	295 (3380)	261 (8250)
$[Cu(bipa)Cl]PF_6$ (**5**)	1054 (133)	820 (98)	290 (3680)	260 (4510)
$[Cu(tmima)Cl]PF_6$ (**6**)	1123 (112)	830 (98)	288 (4560)	
$[Cu(tpa)(1\text{-MeIm})](PF_6)_2$ [c]	793 (177)			256 (12600)
$[Cu(bpia)(1\text{-MeIm})](PF_6)_2$ (**7**)	840 (187)		280(sh) (2200)	256 (9430)
$[Cu(bipa)(1\text{-MeIm})](PF_6)_2$ (**8**)	877 (145)	700 (68)	290(sh) (1860)	261 (5590)
$[Cu(tmima)(1\text{-MeIm})](PF_6)_2$ (**9**)	925 (159)	715 (64)		268 (2250)

[a]In CH_3CN. [b]ϵ, M^{-1} cm^{-1}. [c]Ref. 10.

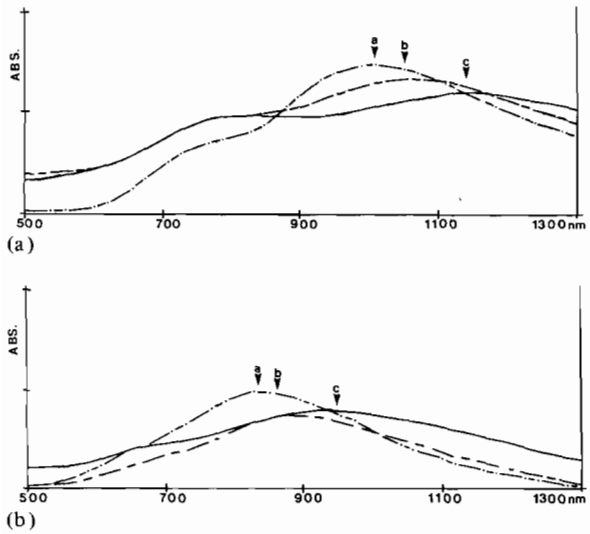

Fig. 5. Electronic spectra: (a) a, $[Cu(bpia)Cl]^+$; b, $[Cu(bipa)Cl]^+$; c, $[Cu(tmima)Cl]^+$; (b) a, $[Cu(bpia)(1\text{-MeIm})]^{2+}$; b, $[Cu(bipa)(1\text{-MeIm})]^{2+}$; c, $[Cu(tmima)(1\text{-MeIm})]^{2+}$.

$Cl]^+$ [5b, 10] these transitions occur at higher energies centered at 962 ($\epsilon = 201\ M^{-1}\ cm^{-1}$) and 736 ($\epsilon = 92\ M^{-1}\ cm^{-1}$) nm. The tris-benzimidazole complex, $[Cu(NTB)Cl]^+$, on the other hand, displays two transitions at 1176 ($\epsilon = 101\ M^{-1}\ cm^{-1}$) and 870 ($\epsilon = 55\ M^{-1}\ cm^{-1}$) nm [7b]. The data suggest, therefore, that the ligand field strength of the tripods decrease as pyridine is replaced with 1-methylimidazole donors and that 1-methylimidazole is a slightly stronger base than benzimidazole. The mixed-ligand complexes **4** and **5** corroborate these results, displaying transitions at 1003 ($\epsilon = 141\ M^{-1}\ cm^{-1}$) and 780 ($\epsilon = 71\ M^{-1}\ cm^{-1}$) nm and 1054 ($\epsilon = 133\ M^{-1}\ cm^{-1}$) and 820 ($\epsilon = 98\ M^{-1}\ cm^{-1}$) nm, respectively. A similar shift of the transitions to lower energies as imidazoles are substituted for pyridines is observed in the ligand field strengths of compounds **7**–**9** (Table 5). The absorption maxima associated with the $[Cu(L)(1\text{-MeIm})]^{2+}$ complexes, however, occur at higher energies than their $[Cu(L)Cl]^+$ counterparts, reflecting the greater ligand field strength of 1-methylimidazole compared to Cl^-.

Magnetic Measurements

Magnetic moments of the complexes were measured at ambient temperatures in acetonitrile solutions according to the Evans method [15]. The magnetic moments fall within the range 1.9–2.0 μ_B (Table 6), as expected for five-coordinate Cu^{II} complexes.

Electron Paramagnetic Resonance Spectroscopy

The X-band EPR spectra of powdered samples of **4**–**9** have been recorded at liquid nitrogen temperatures and their spectral parameters compared to those of $[Cu(tpa)Cl]^+$ and $[Cu(tpa)(1\text{-MeIm})]^{2+}$. $[Cu(tpa)Cl]^+$ displays a spectrum typical of trigonal bipyramidal complexes [27], where $g_\perp \gg g_\parallel \cong 2.0$ and $|A|$ is in the range of $60-100 \times 10^{-4}\ cm^{-1}$ [28]. For compound **4**, three g values are observed: $g_1 = 2.04$, $g_2 = 2.13$, $g_3 = 2.24$, consistent with a rhombic distortion of the complex. The spectra of compounds **5** and **6** are very broad. The parallel region of the spectrum of **5** is poorly resolved while no signal could be resolved in this region for **6**. Apparently, these compounds are not magnetically dilute enough to resolve individual g components.

The EPR spectral parameters of complexes **4**–**9** are compiled in Table 6. In frozen DMF/CH_3OH solutions (77 K), compounds **4**–**6** exhibit spectra typical of trigonal bipyramidal complexes. Analysis of complex $[Cu(bpia)Cl]PF_6$, at 77 K gives parameters of $g_\perp = 2.20$ and $A_\perp = 93 \times 10^{-4}\ cm^{-1}$, consistent with the reported values for $[Cu(tpa)Cl]^+$, $g_\perp = 2.19$ and $A_\perp = 96 \times 10^{-4}\ cm^{-1}$ [5b, 10]. The spectrum appears to be axial, however, due to the absence of resolvable copper hyperfine structure in the parallel region, accurate $g_\parallel$ and $A_\parallel$ values could not be determined. It has been suggested [10] that the spectrum of $[Cu(tpa)Cl]^+$ may be rhombic [10], where the two components of the $g_\perp$ region are close in value. We do not see evidence for splitting in the $g_\perp$ region of the frozen DMF/CH_3OH spectrum of $[Cu(tpa)Cl]^+$ but do notice splitting in the $g_\perp$ region of complexes **4**–**6** (see 'Supplementary Material').

Of the four $[Cu(L)Cl]^+$ complexes studied, **6** displays the largest value for $g_\perp$ (2.25) and the largest copper hyperfine coupling ($A_\perp = 105 \times 10^{-4}\ cm^{-1}$).

TABLE 6. Magnetic moment and EPR data

No.	Complex	μ [a]	Solvent[b]	$g_\parallel$	$g_\perp$	$\lvert A_\parallel \rvert$ [c]	$\lvert A_\perp \rvert$ [c]
4	$[Cu(bpia)Cl]PF_6$	1.95	DMF/CH_3OH		2.20		93
5	$[Cu(bipa)Cl]PF_6$	1.91	DMF/CH_3OH		2.24		105
6	$[Cu(tmima)Cl]PF_6$	1.94	DMF/CH_3OH		2.25		105
7	$[Cu(bpia)(1\text{-MeIm})](PF_6)_2$	1.96	CH_3CN/CH_3OH	2.02	2.18	84	103
8	$[Cu(bipa)(1\text{-MeIm})](PF_6)_2$	1.99	CH_3CN/CH_3OH	2.00	2.19	82	93
9	$[Cu(tmima)(1\text{-MeIm})](PF_6)_2$	1.98	CH_3CN/CH_3OH	2.02	2.21	75	107

[a]300 K, μ_B. [b]Ratio of DMF/CH_3OH = 1:3; ratio of CH_3CN/CH_3OH = 1:3. [c]$|A| \times 10^{-4}\ cm^{-1}$.

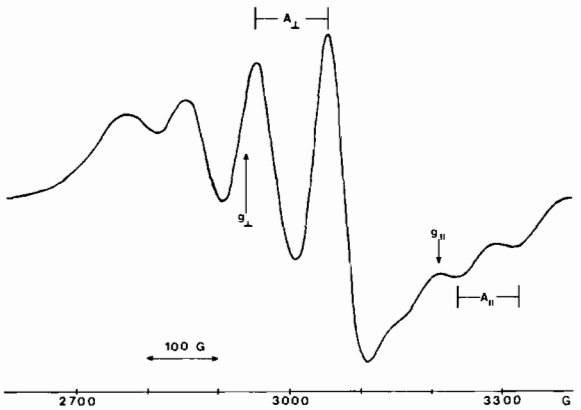

Fig. 6. X-band EPR spectrum of a frozen CH_3CN/CH_3OH solution containing $[Cu(bipa)(1\text{-MeIm})]^{2+}$ at 77 K.

From the complexity of the $g_\perp$ signal, we conclude that **6** has the greatest distortion from trigonal bipyramidal geometry. This is consistent with the crystal structure of **6** (*vide infra*) which has the longest Cu–N(amine) bond distance and the greatest deviations in the trigonal bond angles. As with the spectra of **4** and **5**, the absence of copper hyperfine splitting in the parallel region, precludes accurate determination of $g_\parallel$ and $A_\parallel$.

For complexes **7–9**, the frozen CH_3CN/CH_3OH X-band EPR spectra (77 K) give $g_\perp$ and $g_\parallel$ values indicative of axially distorted trigonal bipyramidal complexes. A spectrum of **8** is shown in Fig. 6. Copper hyperfine splitting is observed in the parallel region of the spectrum allowing $g_\parallel$ and $A_\parallel$ to be determined accurately. For **8**, $g_\perp = 2.19$, $g_\parallel = 2.0$, $A_\perp = 93 \times 10^{-4}$ cm^{-1} and $A_\parallel = 82 \times 10^{-4}$ cm^{-1}. The values of $|A|$ are within the range ($60–100 \times 10^{-4}$ cm^{-1}) reported for other trigonal bipyramidal complexes [10, 28]. The perpendicular region of the spectra of **7–9** are not split as observed for compounds **4–6**, indicating that the $[Cu(L)(1\text{-MeIm})]^{2+}$ complexes are less distorted than their $[Cu(L)Cl]^+$ analogs.

Electrochemistry

The redox properties of compounds **4–9** in acetonitrile solutions are summarized in Table 7 along with data for $[Cu(tpa)Cl]^+$ and $[Cu(tpa)(1\text{-MeIm})]^{2+}$. All of the compounds studied display a single quasi-reversible one-electron reduction step. The peak-to-peak separation of the voltammograms range from 90 to 150 mV and the ratio of peak currents, i_{pa}/i_{pc}, were found to be unity. $[Cu(tmima)Cl]^+$ (**6**) is reduced at a potential of −0.187 V versus NHE. The mixed-ligand compounds **4** and **5** are reduced at −0.273 and 0.207 V versus NHE, respectively, while $[Cu(tpa)Cl]^+$ is reduced at −0.290 V versus NHE. (It has previously been reported that $[Cu(tpa)Cl]^+$ gives a quasi-reversible redox wave with $E_{1/2} = -0.39$ V versus NHE in DMF solvent using a glassy-carbon working electrode.) These results suggest that the tripodal ligands containing imidazole pendants are weaker field ligands than tpa, an observation already noted in the analysis of electronic spectral properties of compounds **4–6**. The anodic shift in the redox properties of the $[Cu(L)Cl]^+$ complexes also indicates that as pyridines are replaced by 1-methylimidazoles the coordination environment of the complexes becomes progressively softer, enhancing the stabilization of the Cu^I ion formed upon reduction. A similar anodic shift of the redox potentials has been observed for $[Cu(tepa)Cl]^+$, which contains six-membered chelate rings [10]. The more flexible six-membered ring size favors the stabilization of the Cu^I ion and the tetrahedral coordination environment observed for $[Cu(tepa)Cl]^+$ [10].

TABLE 7. Electrochemical data for all the complexes[a]

Complex $[Cu(L)Cl](PF_6)$	ΔE (mV)	$E_{1/2}$ vs. NHE (V)
$[Cu(tpa)Cl]PF_6$	110	−0.290
$[Cu(bpia)Cl]PF_6$ (**4**)	120	−0.273
$[Cu(bipa)Cl]PF_6$ (**5**)	130	−0.207
$[Cu(tmima)Cl]PF_6$ (**6**)	120	−0.187
$[Cu(L)(1\text{-MeIm})](PF_6)_2$		
$[Cu(tpa)(1\text{-MeIm})](PF_6)_2$	120	−0.250
$[Cu(bpia)(1\text{-MeIm})](PF_6)_2$ (**7**)	150	−0.237
$[Cu(bipa)(1\text{-MeIm})](PF_6)_2$ (**8**)	135	−0.194
$[Cu(tmima)(1\text{-MeIm})](PF_6)_2$ (**9**)	90	−0.147

[a]In CH_3CN; 1×10^{-4} M in complex and in ferrocene [14]; reference Ag/AgCl electrode; working and auxiliary electrodes are platinum wires; scan rate 20 mV/s.

At the present time the nature of the Cu^I species generated upon reduction of the $[Cu(L)Cl]^+$ complexes is not known. Pentacoordinate Cu^I complexes have been prepared where one or more of the ligands are 'soft', however an overwhelming number of Cu^I complexes, such as $[Cu(tepa)]^+$, appear to be tetrahedral [29]. It is conceivable that one of the pendant ligands or the tertiary amine nitrogen is not bonded to the Cu^+ ion upon reduction. The structure of $[Cu(bipa)Cl]^+$ shows a significant (0.120 Å) lengthening of the Cu–N6(pyridine) bond compared to the Cu–N(imidazole) bond lengths, and a long Cu–N(amine) bond length intermediate between the lengths observed for **6** and $[Cu(tpa)Cl]^+$ [10].

In general, imidazole has been found to be a poorer π-acceptor and better π-donor ligand, when compared to pyridine [30]. In addition, imidazole is a pseudo-aromatic molecule and a 'borderline' base as defined by the HSAB theory [31]. E and C values for 1-methylimidazole suggest that it is a stronger

base than pyridine with 'softer' properties [32]. The ligand field strength of the tetrahedral environment, would be dominated by the base strength of the heterocyclic π bonding ligands. As a result, the redox properties of the Cu^{II} complexes are expected to shift to more anodic potentials as the tripodal ligands become progressively 'softer' (i.e. tpa < bpia < bipa < tmima).

For the $[Cu(L)(1\text{-MeIm})]^{2+}$ complexes, **7**–**9**, a similar anodic shift in redox potentials is observed. $[Cu(tmima)(1\text{-MeIm})]^{2+}$ is reduced at −0.147 V versus NHE while the mixed ligand complexes **7** and **8** are reduced at −0.237 and −0.194 V versus NHE, respectively. $[Cu(tpa)(1\text{-MeIm})]^{2+}$, under the conditions of our electrochemical measurements, is reduced at −0.250 V versus NHE. If the same metal–ligand bond scission mechanism occurs upon reduction of the $[Cu(L)(1\text{-MeIm})]^{2+}$ complexes, then the anodic shift in the reduction potentials of **5**–**7** are a reflection of the 'softer' nature of 1-methylimidazole as a base compared to the Cl^-.

Conclusions

Understanding how ligands fine-tune the structural, spectroscopic and electrochemical properties in copper complexes is important in order to ascertain the factors required in stabilizing Cu^{I} and Cu^{II} forms of copper proteins. We have prepared a series of tripodal ligands, designated L, where L = bpia (**1**), bipa (**2**) and tmima (**3**), and observed a systematic variance in their structural and electronic properties. The structures and properties of compounds **4**–**9** have been compared with two previously reported tripodal complexes, $[Cu(tpa)Cl]^+$ and $[Cu(tpa)(1\text{-MeIm})]^{2+}$ [5b, 10], in order to generate structurally related compounds containing from zero to three imidazole donors. Complexes **5** and **6** have been characterized by X-ray crystallography and shown to have copper centers with distorted trigonal bipyramidal geometries. Distortion of the coordination environments increases as the number of imidazole donors are increased. Most notable distortions in the geometries of the complexes are reflected in decreases in the chelate bond angles, concomitant with increases in the Cu–N(amine) bond lengths. The EPR spectral data for the complexes are consistent with these distortions, with $[Cu(tmima)Cl]^+$ and $[Cu(tmima)(1\text{-MeIm})]^{2+}$ having the largest, average g and $|A|$ values. The electronic and electrochemical properties of the $[Cu(L)Cl]^+$ and $[Cu(L)(1\text{-MeIm})]^{2+}$ complexes indicate that the 1-methylimidazole pendants are weaker field ligands than pyridine pendants and that the donor strength follows the series' tpa < bpia < bipa < tmima.

Supplementary Material

Anisotropic thermal parameters, bond distances, bond angles, H atom parameters, bond lengths and angles, parameters of the disordered PF_6 and structure factors are collected in Tables S1–S15. These Tables as well as Figures showing solution EPR spectra of complexes **4**–**9** are available from the authors on request.

Acknowledgements

We are thankful for the support of the National Science Foundation (Grant RII-8610671) and the Commonwealth of Kentucky through the Kentucky EPSCoR program (R.M.B.)

References

1 (a) C. A. Evans, R. Guevremont and D. L. Rabenstein, *Metal Ions Biol. Syst., 9* (1979) 41; (b) H. C. Freeman, in G. L. Eichhorn (ed.), *Inorganic Biochemistry*, Vol. 1, Elsevier, Amsterdam, 1973, p. 121; (c) M. E. Winkler, K. Lerch and E. I. Solomon, *J. Am. Chem. Soc., 103* (1981) 7001.

2 (a) W. P. J. Gaykema, W. G. J. Hol, J. M. Vereijken, N. M. Soeter, H. J. Bak and J. J. Beintema, *Nature (London), 309* (1984) 23; (b) E. I. Solomon, K. W. Penfield and D. E. Wilcox, *Struct. Bonding (Berlin), 53* (1983) 1.

3 (a) H. B. Gray and E. I. Solomon, in T. G. Spiro (ed.), *Copper Proteins*, Wiley, New York, 1981, pp. 1–39; (b) K. D. Karlin and J. Zubieta, *Inorg. Persp. Biol. Med., 2* (1979) 127; (c) P. M. Colman, H. C. Freeman, J. M. Guss, M. Murata, V. A. Norris, J. A. M. Ramshaw and M. P. Venkatappa, *Nature (London), 272* (1978) 319; (d) E. T. Adman, R. E. Stenkamp, L. C. Sieker and L. H. Jensen, *J. Mol. Biol., 123* (1978) 35; (e) H. S. Mason, in K. T. Yasunobu, H. F. Mower and O. Hayaishi (eds.), *Iron and Copper Proteins*, Plenum, New York, 1970, p. 464.

4 K. D. Karlin and J. Zubieta (eds.), *Copper Coordination Chemistry: Biochemical and Inorganic Perspectives*, Adenine, New York, 1983.

5 (a) K. D. Karlin, J. C. Hayes, J. P. Hutchinson, J. R. Hyde and J. Zubieta, *Inorg. Chim. Acta, 64* (1982) L219; (b) K. D. Karlin, J. C. Hayes, S. Juen, J. P. Hutchinson and J. Zubieta, *Inorg. Chem., 21* (1982) 4106; (c) K. D. Karlin, P. L. Dahlstrom, J. C. Hayes, R. A. Simon and J. Zubieta, *Cryst. Struct. Commun., 11* (1982) 907; (d) R. R. Jacobson, Z. Tyeklar, A. Farooq, K. D. Karlin, S. Liu and J. Zubieta, *J. Am. Chem. Soc., 110* (1988) 3690.

6 (a) F. Mani, *Inorg. Nucl. Chem. Lett., 17* (1981) 45; (b) T. N. Sorrell and D. L. Jameson, *Inorg. Chem., 21* (1982) 1014; (c) G. J. Kleywegt, W. G. R. Wiesmeijer, G. J. Van Driel, W. L. Driessen, J. Reedijk and J. H. Noordik, *J. Chem. Soc., Dalton Trans.*, (1985) 2177.

7 (a) H. M. J. Hendriks, P. J. M. W. L. Birker, G. C. Verschoor and J. Reedijk, *J. Chem. Soc., Dalton Trans.*, (1982) 623; (b) A. W. Addison, H. M. J. Hendriks, J. Reedijk and L. K. Thompson, *Inorg. Chem., 20* (1981) 20; (c) L. K. Thompson, B. S. Ramaswamy and R. D. Dawe, *Can. J. Chem., 56* (1978) 1311.

8 B. A. Averill, A. P. Chandhuri, D. C. Hendrix and H. C. Silvis, *Cienc. Biol. (Portugal), 5* (1981) 167.
9 R. R. Jacobson, Z. Tyeklar, K. D. Karlin and J. Zubieta, *3rd Chemical Congr. of North America, Toronto, Canada, 1988,* Abstr. no. INOR 554.
10 J. Zubieta, K. D. Karlin and J. C. Hayes, in K. D. Karlin and J. Zubieta (eds.), *Copper Coordination Chemistry: Biochemical and Inorganic Perspectives,* Adenine, New York, 1983, pp. 97–108.
11 K. Takahashi, E. Ogawa, N. Oishi, Y. Nishida and S. Kida, *Inorg. Chim. Acta, 66* (1982) 97.
12 J. Whelan and B. Bosnich, *Inorg. Chem., 25* (1986) 3671.
13 A. J. Bard and L. R. Faulkner, *Electrochemical Methods, Fundamentals and Applications,* Wiley, New York, 1980, Ch. 6.
14 R. R. Gagné, C. A. Koval and G. C. Lisensky, *Inorg. Chem., 19* (1980) 2855.
15 R. A. Bailey, *J. Chem. Educ., 49* (1972) 297.
16 F. Højland, H. Toftlund and S. Yde-Anderson, *Acta Chem. Scand., Ser. A, 37* (1983) 251.
17 K. J. Oberhausen, J. F. Richardson, R. M. Buchanan and W. Pierce, *Polyhedron, 5* (1989) 659.
18 M. Di Vaira, F. Mani and P. Stoppioni, *J. Chem. Soc., Chem. Commun.,* (1989) 126.
19 B. A. Frenz, The Enraf-Nonius CAD4 SDP, a real-time system for concurrent X-ray data collection and crystal structure determination, in H. Schenk, R. Olthof-Hazelkamp, H. van Konigsveld and G. C. Bassi (eds.), *Computing in Crystallography,* Delft University Press, Delft, The Netherlands, 1978, pp. 64–71.
20 R. C. B. G. Killean and J. L. Lawrence, *Acta Crystallogr., Sect. B, 25* (1969) 1750.
21 D. T. Cromer and J. T. Waber, *International Tables for X-ray Crystallography,* Vol. IV, Kynoch Press, Birmingham, U.K., 1974, Table 2.2B.
22 J. A. Ibers and W. C. Hamilton, *Acta Crystallogr., 17* (1964) 781.
23 D. T. Cromer, *International Tables for X-ray Crystallography,* Vol. IV, Kynoch Press, Birmingham, U.K., 1974, Table 2.3.1.
24 E. L. Muetterties and L. J. Guggenberger, *J. Am. Chem. Soc., 96* (1974) 1748.
25 (a) T. N. Doman, J. F. Richardson, L. Arar and R. M. Buchanan, *Inorg. Chim. Acta, 159* (1989) 219; (b) R. S. Glass, M. Sabahi, M. Hojjatie and G. S. Wilson, *Inorg. Chem., 26* (1987) 2194; (c) U. Geiser, B. L. Ramakrishna, R. D. Willett, F. B. Hulsbergen and J. Reedijk, *Inorg. Chem., 26* (1987) 3750; (d) E. Bernarducci, P. K. Bharadwaj, K. Krogh-Jespersen, J. A. Potenza and H. J. Schugar, *J. Am. Chem. Soc., 105* (1983) 3860.
26 M. Duggan, N. Ray, B. Hathaway, G. Tomlinson, P. Brint and K. Pelin, *J. Chem. Soc., Dalton Trans.,* (1980) 1342.
27 B. J. Hathaway and D. E. Billing, *Coord. Chem. Rev., 5* (1970) 143.
28 A. Bencini, I. Bertini, D. Gatteschi and A. Scozzafava, *Inorg. Chem., 17* (1978) 3194.
29 (a) A. W. Addison, M. Carpenter, L. K.-M. Lau and M. Wicholas, *Inorg. Chem. 17* (1978) 1545; (b) R. R. Gagné, J. L. Allison, R. S. Gall, and C. A. Koval, *J. Am. Chem. Soc., 99* (1977) 7170.
30 (a) C. R. Johnson and R. E. Shepherd, *Inorg. Chem., 22* (1983) 3506; (b) C. R. Johnson, W. W. Henderson and R. E. Shepherd, *Inorg. Chem., 23* (1984) 2754; (c) C. M. Jones, C. R. Johnson, S. A. Asher and R. E. Shepherd, *J. Am. Chem. Soc., 107* (1985) 3772.
31 R. G. Pearson, *Science (Washington, DC), 151* (1966) 172.
32 R. L. Courtright, R. S. Drago, J. A. Nusz and M. S. Nozari, *Inorg. Chem., 12* (1973) 2809.